

Electronic Supplementary Information

***In situ* formation of porous LiCuVO₄/LiVO₃/C nanotubes as high-capacity anode material for lithium ion batteries**

Rong Cui^a, Jiande Lin^a, Xinxin Cao^a, Pengfei Hao^a, Xuefang Xie^a, Shuang Zhou^a, Yaping Wang^a, Shuquan Liang^{a,b} and Anqiang Pan^{a,b,*}

^a School of Materials Science & Engineering, Central South University, Changsha 410083, Hunan, China

^b Key Laboratory of Nonferrous Metal Materials Science and Engineering, Ministry of Education, Central South University, Changsha 410083, Hunan, China

* Corresponding author: pananqiang@csu.edu.cn (A.Q. Pan)

Table of Contents

Figure S1 The X-ray diffraction pattern of LCVO-500.....	S1
Figure S2. Raman scattering spectra of the LCVO-450, LCVO-250 and LCVO-precursor.....	S1
Figure S3. TG/DSC curve of the LCVO-500 annealed from room temperature to 650 °C at a temperature ramping rate of 10 °C min ⁻¹ in air.....	S2
Figure S4. The FESEM images of LCVO-500 at low and high magnifications.....	S2
Figure S5. The rate performance of the LCVO-450 electrode with high mass loading (1.32 mg cm ⁻²)	S3
Figure S6. SEM images of (a) LCVO-450 electrode, and (b) LCVO-450 powder after ultrasonic dispersion after rate-capability tests at various current densities from 0.1 to 2 A g ⁻¹	S3
Table S1. Refined unit cell lattice parameters of LiCuVO ₄ and LiVO ₃ in LiCuVO ₄ /LiVO ₃ /C and the standard data of LiCuVO ₄ (15836-ICSD) and LiVO ₃ (2899-ICSD)	S4
Table S2. Electrochemical performance comparison of LiCuVO ₄ , LiVO ₃ and relevant materials for lithium ion batteries.....	S4

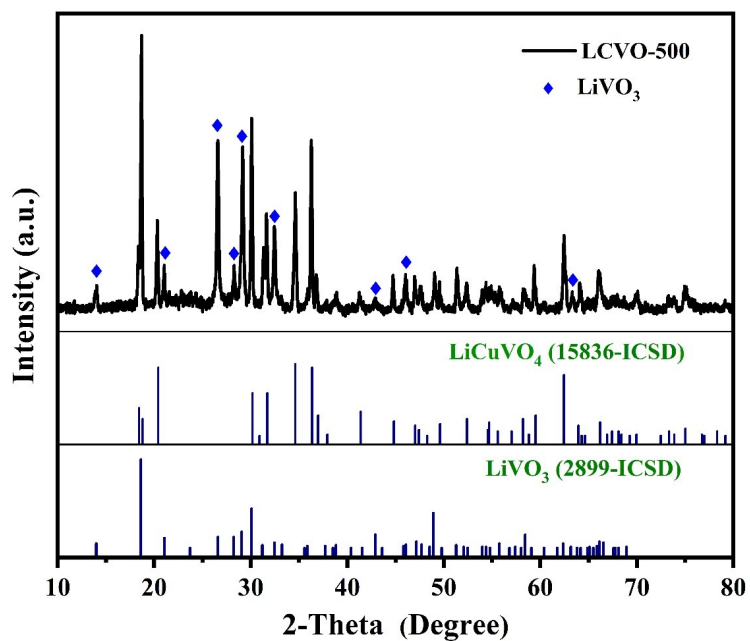


Figure S1 The X-ray diffraction pattern of LCVO-500.

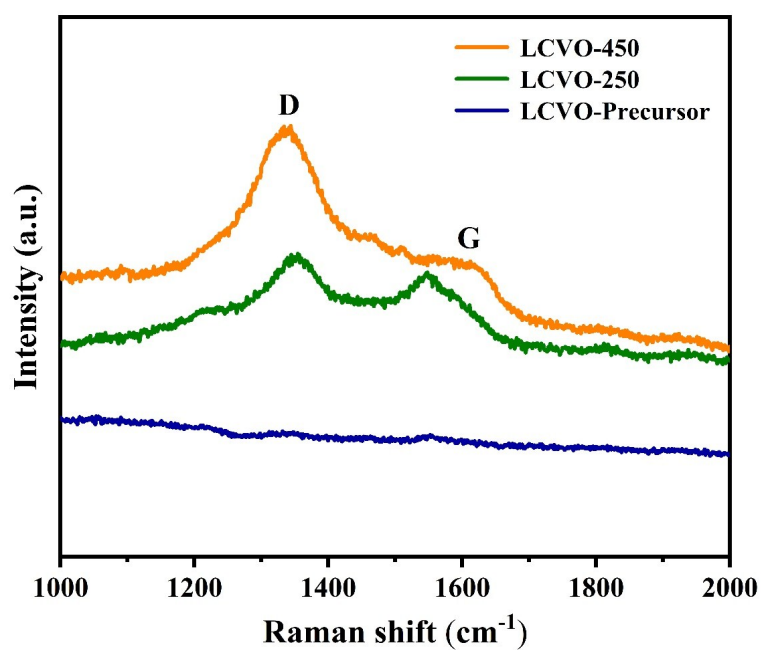


Figure S2. Raman scattering spectra of the LCVO-450, LCVO-250 and LCVO-precursor.

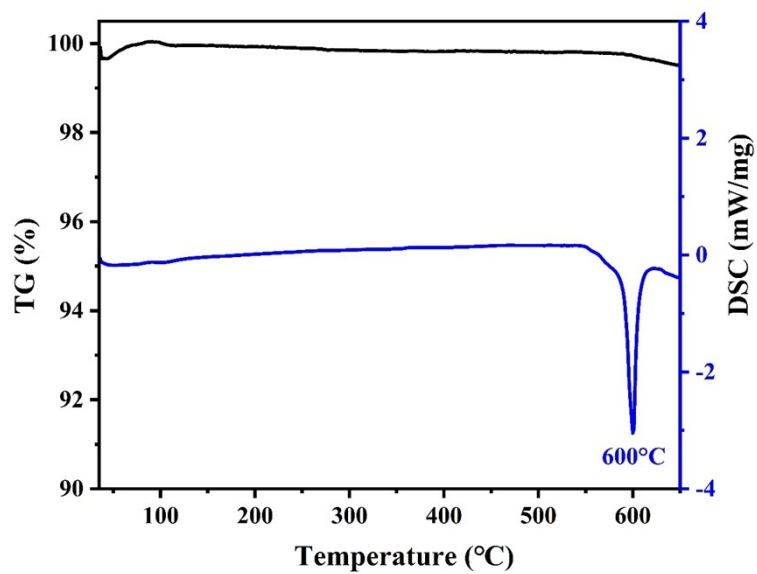


Figure S3. TG/DSC curve of the LCVO-500 annealed from room temperature to 650 °C at a temperature ramping rate of 10 °C min⁻¹ in air.

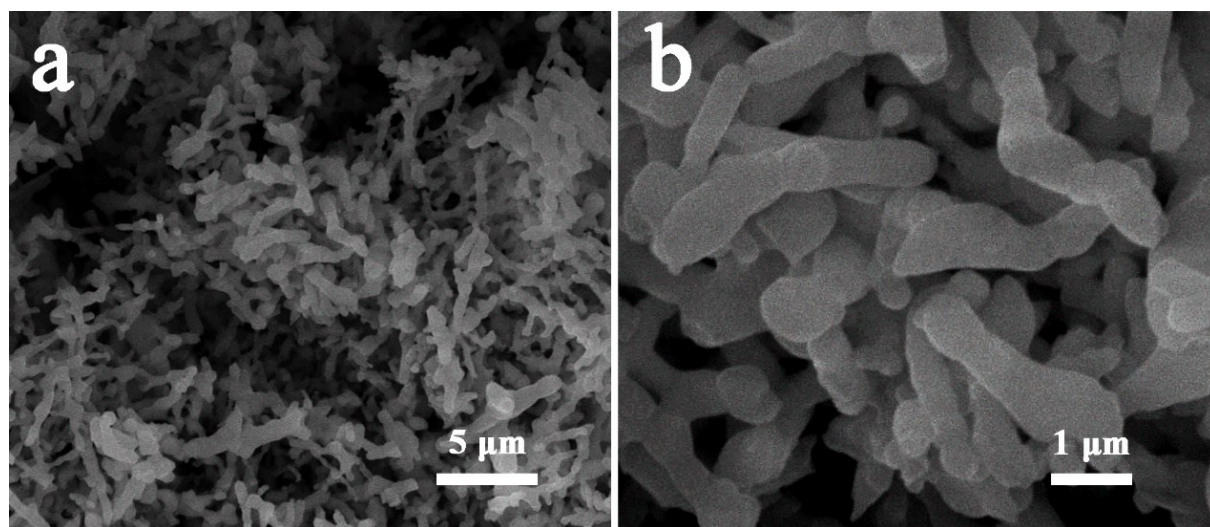


Figure S4. The FESEM images of LCVO-500 at low and high magnifications.

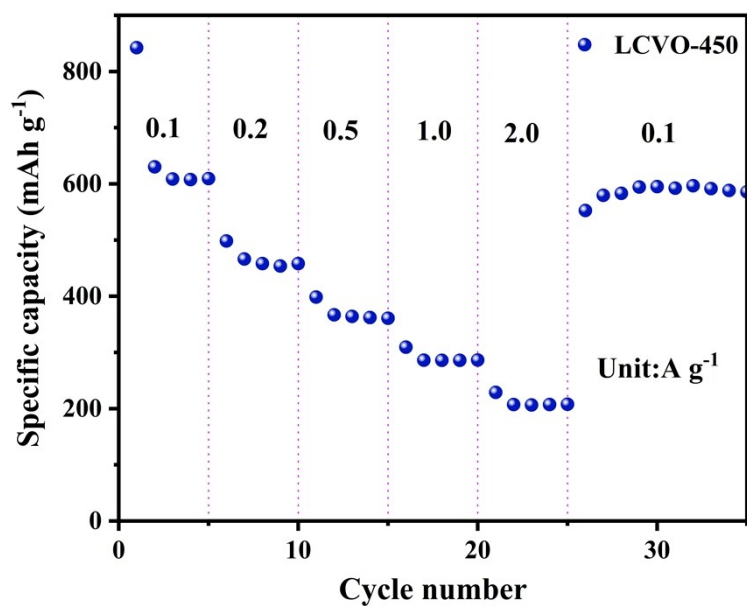


Figure S5. The rate performance of the LCVO-450 electrode with high mass loading (1.32 mg cm⁻²).

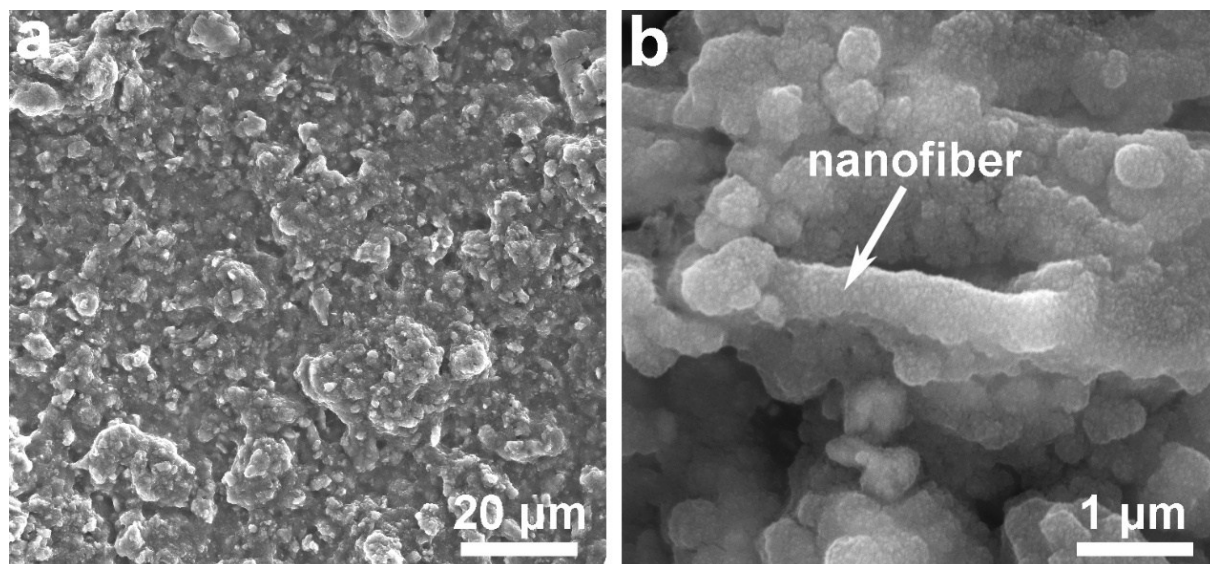


Figure S6. SEM images of (a) LCVO-450 electrode, and (b) LCVO-450 powder after ultrasonic dispersion after rate-capability tests at various current densities from 0.1 to 2 A g⁻¹.

Table S1. Refined unit cell lattice parameters of LiCuVO₄ and LiVO₃ in LiCuVO₄/LiVO₃/C and the standard data of LiCuVO₄ (15836-ICSD) and LiVO₃ (2899-ICSD).

sample	Lattice parameters					Phase content (wt%)	Evaluation parameters		
	a (nm)	b (nm)	c (nm)	β (°)	V (nm ³)		Rwp (%)	Rp (%)	CHI ² (%)
LiCuVO ₄ in LCVO-450	0.5658	0.58087	0.87139	90.0000	0.28637	24.6	9.62	7.56	4.44
LiCuVO ₄	0.5652	0.58100	0.87500	90.0000	0.28733	—	—	—	—
LiVO ₃ in LCVO-450	1.0153	0.84377	0.58837	110.4740	0.47223	75.4	9.62	7.56	8.33
LiVO ₃	1.0158	0.84175	0.58853	110.4800	0.47142	—	—	—	—

Table S2 Electrochemical performance comparison of LiCuVO₄, LiVO₃ and relevant materials for lithium ion batteries.

Samples	Current density (mA g ⁻¹)	Cycle number (n)	Capacity (mA h g ⁻¹)	Initial Capacity (mA h g ⁻¹)
LiCuVO ₄ powder ¹	200	50	~400	680
Interconnected LiCuVO ₄ networks ²	100	50	~580	875
LiVO ₃ ³	100	50	~700	1300
Li ₃ VO ₄ /C/rGO ⁴	50	200	~387	712
Li ₃ VO ₄ /C ⁵	400	100	~394	570
LCVO-450	100	50	~576	910

References

1. M. Li, X. Yang, C. Wang, N. Chen, F. Hu, X. Bie, Y. Wei, F. Du and G. Chen, *J. Mater. Chem. A*, 2015, **3**, 586-592.
2. L. Wang, Y. Dong, K. Zhao, W. Luo, S. Li, L. Zhou and L. Mai, *Phys. Chem. Chem. Phys.*, 2017, **19**, 13341-13347.
3. J. Lee, J. Moon, O. Chae, J. Lee, J. Ryu, M. Cho, K. Cho and S. Oh, *Chem. Mater.*, 2016, **28**, 5314-5320.
4. Y. Yang, J. Li, J. Huang, J. Huang, J. Zeng and J. Zhao, *Electrochim. Acta*, 2017, **247**, 771-778.
5. Z. Liang, Z. Lin, Y. Zhao, Y. Dong, Q. Kuang, X. Lin, X. Liu and D. Yan, *J. Power Sources*, 2015, **274**, 345-354.